Hindawi
Advances in Materials Science and Engineering
Volume 2021, Article ID 4986245, 10 pages
https://doi.org/10.1155/2021/4986245

Research Article

Research on Prediction Model of Prestress Loss of Anchor Cable in Soil-Rock Dual-Structure Slope

Xuhe Gao,[1] **Weiping Tian**,[2] **Jiachun Li**,[2] **Hongliang Qi**,[2] **and Zhipei Zhang**[3]

[1]*School of Mechanics, Civil Engineering & Architecture, Northwestern Polytechnical University, Xi'an, Shaanxi 710129, China*
[2]*Key Laboratory of Highway Engineering in Special Region, Ministry of Education, Chang'an University, Xi'an, Shaanxi 710064, China*
[3]*College of Geology and Environment, Xi'an University of Science and Technology, Xi'an, Shaanxi 710054, China*

Correspondence should be addressed to Xuhe Gao; 81706037@qq.com

Received 4 August 2021; Accepted 29 September 2021; Published 19 October 2021

Academic Editor: Ivan Giorgio

Copyright © 2021 Xuhe Gao et al. This is an open access article distributed under the Creative Commons Attribution License, which permits unrestricted use, distribution, and reproduction in any medium, provided the original work is properly cited.

The establishment of the prestressed cable loss prediction model is a difficult problem faced by the popularization and use. This article aims at the problem of the loss of anchor cable prestress over time in the soil-rock dual-structure slope. We relied on the soil-rock dual-structure slope treatment project of section K5 + 220-K5 + 770 of Jiangwen Expressway and monitored the prestress loss of the anchor cable in the slope through the anchor cable meter with built-in vibrating wire sensor. Using regression analysis and segmented modelling methods, we established a comprehensive mathematical improvement model, analyzed the applicability of the improved model, and obtained the error range, 0.04%–8.9%. This work offers a new approach for predicting anchor cable prestress loss, which has certain practical value for the use of prestressed anchor cables.

1. Introduction

Slopes composed of an upper gravel soil layer and lower weathered bedrock layer are known as soil-rock dual-structure slopes. Engineering projects are typically difficult to implement on soil-rock dual-structure slopes, as poor design or construction work can easily lead to geological failures, such as landslides and slope collapses, which can threaten the safety of the project. To address these challenges, antislide piles and anchor cables are widely used in slope support and reinforcement structures because they can bear some of the sliding force of the slope and help prevent geological failure. However, due to the complexity of engineering geological conditions and the relaxation of the anchor cable itself, it is difficult to calculate the prestress loss of the anchor cable. Therefore, grasping the short-term and long-term prestress loss of anchor cables and quantifying the prestress loss of anchor cables have become a necessary research content.

Li et al. [1] used a contact friction interface element to analyze the interaction and coupling between a simulated anchor cable, slurry, and rock interface. In that study, numerical simulation was used to analyze the mechanical mechanisms and reinforcement effect of a single anchor cable. More significantly, other studies have provided innovative approaches to solving the challenges associated with prestressed anchor cables. However, the problem of prestress dissipation over time has not been adequately addressed. Brahim and Ballivy [2] conducted a five-year monitoring project on the prestress of nine anchor cables. The measured prestress losses were then divided into three major stages: sharp decline, fluctuating change, and gentle change. Nonetheless, the study did not thoroughly investigate the mechanisms and challenges of prestress loss over time. Based on this prestress loss framework, Brahim et al. [3] then studied the law of anchor cable prestress change and proposed that, in the second half of the change process, the rate of prestress change gradually decreases due to the long-term creep of the anchor cable. The research analyzed the prestress loss directionally and lacked quantitative prediction of the prestress loss law. Xiao [4] examined the changes in anchor cable prestress in the high slope of the Three

Gorges Sluice and verified the reinforcement of the ship lock provided by the prestressed anchor cables. This study also did not involve prediction of prestress losses. Li et al. [5] evaluated the construction quality of rock anchors and provided different perspectives on the effects of anchor cable reinforcement as assessed by the change in anchor cable prestress. Ding and Bai [6] studied prestressed anchor cables used for rock mass reinforcement from a theoretical perspective and classified prestress loss in the rock mass cable into two types of prestress loss: free segment and anchor segment. They concluded that the main loss of anchor cable prestress is caused by the creep of the rock mass in the free and anchor cable segments and the inherent relaxation characteristics of the anchor cable. However, this study also lacks an investigation into the prediction of prestress losses. Chen et al. [7] conducted model tests, examined the creep equations of simulated soft rock materials, and derived an estimation method for anchor cable tonnage loss over time. However, this method is based on assumptions and simplifications; thus, it is insufficient to be used effectively in conjunction with field monitoring data.

In addition, while there is ample literature regarding the analysis of monitoring data, the modelling of anchor cables is less well studied. Zhu et al. [8, 9] analyzed the excavation of an underground cavern group by numerical simulation and proposed an empirical formula for the elastoplastic displacement of the powerhouse side wall accounting for the effects of the excavation. Li et al. [10] implemented the damage rheological coupling model in FLAC3D software, analyzed the fracture failure characteristics of the surrounding rocks during cave excavation, and used the fracture failure criteria to predict the deformation caused by the opening of the crack. The cleavage failure area caused by stress release was also calculated. Wu et al. [11] used the numerical simulation and analyzed monitoring data to study the deformation, failure mechanisms, and stress characteristics of prestressed anchor cable in the rock surrounding Jinping Hydropower Station, which was under high geostress. Wang et al. [12] studied the coupling of anchor cable prestress loss and rock mass creep in underground pump station buildings. In particular, they verified the formula for anchor cable prestress loss calculations and compared and analyzed the differences between the theoretically calculated and the measured values of anchor cable prestress loss. Finally, Cheng et al. [13] analyzed the prestress loss of anchor cables in a rock mass damaged by excavation and unloading under high geostress and rock creep conditions. They also proposed a model for long-term prediction of anchor cable prestress based on the equivalent strain assumption. These studies used numerical simulation methods to analyze the stress and deformation of the prestressed anchor cable and the surrounding rock and soil body according to different site conditions. However, these studies did not establish a model of anchor cable prestress loss.

Therefore, this study aims to address the challenge of predicting anchor cable prestress loss. This study used the monitoring data collected from prestressed anchor cables used for a slope protection engineering project to investigate the phenomenon of prestress loss. In particular, the prestress loss and the prestress change process of the anchor cables were analyzed. Furthermore, regression analysis was used to develop an improved model of prestress loss that was shown to have robust applicability. The results of this research demonstrate that the proposed model can be used to facilitate accurate prediction of on-site prestress loss, overcoming the limitations of previous work in this area.

2. Materials and Methods

2.1. Study Area. This study examined the right slope of the TJ1A K5 + 220–K5 + 770 section of the Jiangwen Expressway Governance project. During the excavation of the slope, tension cracks formed on the ground surface three times. As a result, different degrees of slippage occurred, and construction safety was seriously affected. The first instance occurred on April 3, 2014, when ground cracks formed in the K5 + 680 to K5 + 770 section, causing slope slip. The second instance occurred on June 1, 2014, in the K5 + 540 to K5 + 680 section of the right slope between 30 and 50 m north of the west side. Due to the lack of timely treatment and continuous rainfall, the first landslide continued to develop, which induced a second traction slip. The third occurrence was on September 28, 2014, when ground surface subsidence occurred between K5 + 385 and K5 + 500.

The first support structure was designed for the left and right sides of the K5 + 327 to K5 + 520 section. The grade of the first slope was 1 : 0.75, and it had a height of 8 m and a window-type retaining wall for protection. The second slope had a grade of 1 : 0.75, a slope height of 8 m, and grass planted in a prestressed anchor cable frame for protection. The anchor cable was 20 m long and the anchor was 10 m long. The third slope had a grade of 1 : 1, a slope height of 8 m, and grass planted in a prestressed anchor cable frame for protection. The anchor cable was 20 m long and the anchor was 10 m long. Finally, the fourth slope had a grade of 1 : 1 and reached the top of the slope. The fourth slope was protected by a grass block and a stone grid.

Antisliding piles were added at the third-level platform for additional reinforcement. The cross-sectional dimensions of the antisliding piles were 3×2.4 m, the distance between the piles was 5.0 m, and the length of the piles was 30 m. Three levels of anchor cables were added for slopes 2 and 3. The slope was reinforced every 3 m, and the anchor cable was a 4 Φs 15.24 scattered-type cable with a downward tilt of 20° and a drilling hole diameter of 130 mm. The total length of the anchor cable was 20 m, the anchor section was 10 m long, and the anchor cable prestress was 500 kN.

On September 28, 2014, cracking occurred on the right slope of the K5 + 385 to K5 + 500 section. The cracks were intermittently continuous arcs ranging from a 2–12 m long, 1–3 cm wide, and 0.4–2.0 m deep. The second stage of reinforcement was thus designed and constructed between October 2015 and December 2016 in the K5 + 336 to K5 + 500 section. The cross section of the antisliding piles was $3\,m \times 2.4$ m, and the pile spacing was 5.0 m. An additional anchor beam was added to the top of the antisliding pile using a 6 Φs 15.24 anchor cable tilted 28° downwards with a hole diameter of 130 mm. The antisliding piles were

numbered Z11 to Z17, the length of the anchor cable was 33 m, the anchoring section was 11 m long, and 750 kN of prestress was applied. A row of anchor cable antisliding piles was also added to the secondary platform of the slope, and the tops of the piles were connected by beams. These antisliding piles were 33–34 m long. The pile top anchor cable was a 6 Φs 15.24 dispersion type cable angled 20° downhill with a drilling hole diameter of 130 mm, an anchoring section length of 12 m, and a prestress of 750 kN. The tops of piles Z47 and Z48 were not anchored by cable. The first grade used a window hole-type retaining wall, and the fourth grade used rhombic grid planting grass to protect the slope.

The stratum and support are shown in Figure 1.

2.2. Relevant Geological Conditions

2.2.1. Topography. The study area has the structure and erosion patterns of middle- and low-mountain topography. The elevation of the area is 590–650 m and the slope is 20°–45°. There is growth of natural, slope-protective vegetation on the mountain, and the slope is stable.

2.2.2. Formation Lithology. The strata in this section are predominantly the Lower Cambrian Jindingshan Formation (∈1j) and the Lower Cambrian Qingxudong Formation (∈1q). In the Jindingshan Formation (∈1j), the upper section is light gray calcareous shale interbedded with mudstone. The lower section is sandy shale between shallow clay shale, feldspar quartz sandstone, quartz sandstone, and other minerals. Part of the formation is gray, dark gray, or gray-black thin-thick layered sandstone with carbonaceous shale and mudstone. Strata occurrence is affected by tectonic movement in the area in accordance with the development of folds. The Qingxudong Formation (∈1q) has lithological combinations of limestone, dolomite limestone, and marl intercalated shale, among other features. The appearance of the formation and the development of rock folds, small faults, and joint fissures in this formation are affected by tectonic movement.

2.3. Preliminary Model Assumptions. According to the previous analysis, the long-term loss of anchor cable prestress is mainly caused by the creep of rock and soil; factors such as hole friction and slackening of steel strands have a limited effect on prestress loss and can be mitigated by overtensioning. Therefore, only the loss of prestress due to rock and soil creep was considered for modelling. Many scholars have investigated the rock mass creep failure process, which can be divided into four stages, as shown in Figure 2:

(1) The elastic deformation stage, in which the initial stages of rock and soil deformation occur

(2) The creep deceleration phase, in which creep occurs in the rock and soil, the rate of which decreases over time

(3) The stable creep stage, in which stable creep occurs in the rock and soil, and the creep rate remains effectively unchanged

(4) The accelerated creep phase, in which the creep rate of the rock and soil body increases until damage to the formation occurs

The rock and soil mass subjected to prestressing by an anchor cable can only undergo the first three stages of creep. Thus, the accelerated creep phase was unconsidered in this model. According to the creep law of the rock and soil, the anchor cable prestress loss law was modelled under the following assumptions.

Assumption 1. The elastic modulus of the steel strand is much greater than that of the rock and soil body, and the stiffness and stability of the anchor are much greater than the rigidity and stability of the rock and soil body. The steel strand has only elastic deformation.

Assumption 2. The prestress fluctuations caused by anchor clamping and channel friction during tensioning can be ignored.

Assumption 3. The anchoring of the prestressed anchor cable does not cause fundamental damage to the rock and soil. The anchor cable is in a balanced state after being tensioned and locked.

Under the action of simple stress, A. D. Manasevtsch [14] obtained the relationship between strain and time as follows:

$$\varepsilon_{(t)} = \frac{t}{at + b} + 1, \tag{1}$$

where a and b are experimental constants that depend on the engineering characteristics of the soil.

The prestress of the anchor cable at t is therefore as follows:

$$F_{(t)} = F_0 \exp\left(-\frac{t}{at + b}\right). \tag{2}$$

When $t \longrightarrow \infty$, the final prestress of the anchor cable approaches

$$F_{(t)} = F_0 \exp\left(-\frac{1}{a}\right), \tag{3}$$

where $F_{(0)}$ is the initial prestress and $F(t)$ is the prestress function at time t.

2.4. Anchor Cable Monitoring. An anchor cable meter with integral sealing technology and a stable, high-sensitivity vibrating wire sensor was installed on the hollow pressure-bearing cylinder. Images from the installation and a structural diagram of the meter are shown in Figures 3 and 4, respectively. When a load acts on the anchor cable meter, the deformation of the elastic cylinder is transmitted to the steel string, which deforms accordingly. The electromagnetic coil then excites the deformed steel string and measures its vibration frequency. The frequency signal is transmitted to the

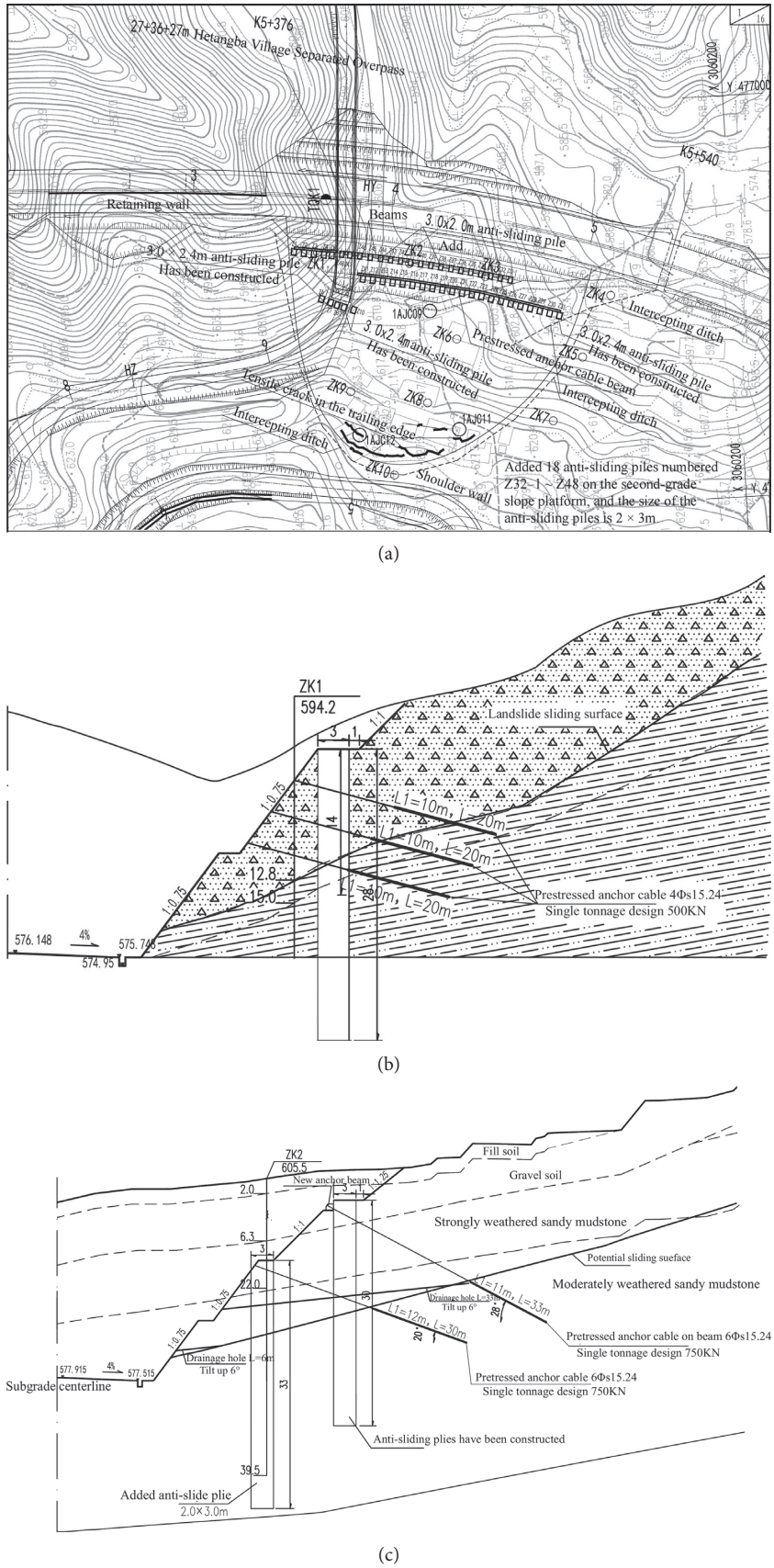

Figure 1: Slope strata and supporting measures with dual structure in the study area. (a) Overall plan of the slope (2016). (b) Cross-sectional view of the slope at K5 + 365 (2014). (c) Cross-sectional view of the slope at K5 + 420 (2016).

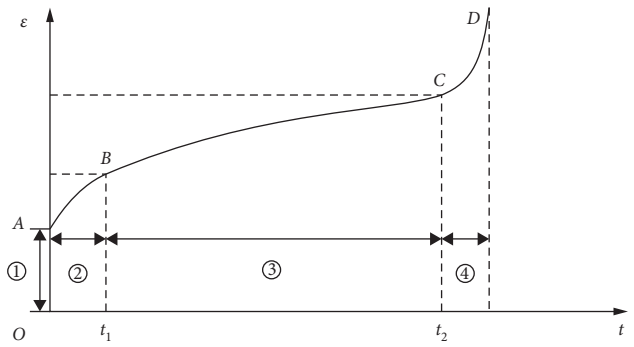

Figure 2: The four stages of rock creep.

(a) (b)

Figure 3: Installation of the anchor cable meter.

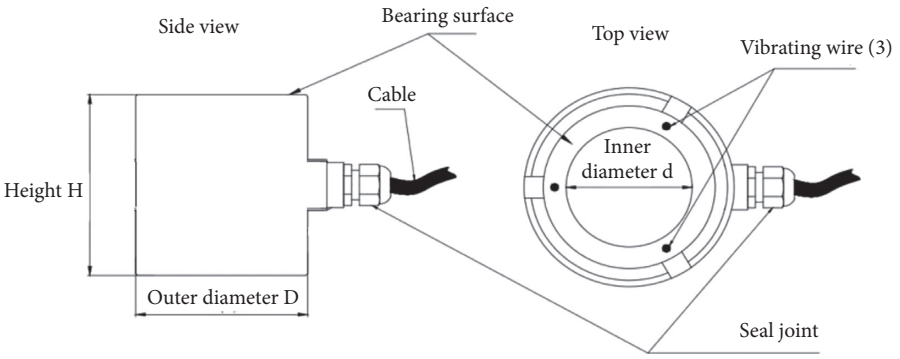

Figure 4: Structural diagram of a vibrating wire anchor cable meter.

vibrating wire reader via a cable, and the frequency input is read and recorded. The recorded frequency can then be used to calculate the load acting on the anchor cable in accordance with the following equation:

$$F = K\frac{\sum_{j=1}^{n}\left(f_{ji}^2 - f_{j0}^2\right)}{n} + K_t\left(T_{ji} - T_{j0}\right), \quad (4)$$

where F is the load on the cable in kN and K is the sensitivity coefficient reflecting the linear relationship between the output frequency of the anchor cable meter and the cable force, which is calibrated at the factory and reported in units of kN/Hz^2. Furthermore, n is the number of strings, f_{ji} is the output frequency of the jth string ($1 \le j \le n$) under the load at time i, f_{j0} is the output frequency of the jth string in the initial state, and K_t is the coefficient describing the relationship between cable force and temperature, which is calibrated upon leaving the factory and reported in units of kN/°C. Finally, T_{ji} is the temperature measured on-site, and T_{j0} is the factory calibration temperature, both in°C.

3. Results

3.1. Monitoring of Anchor Cable Prestress. After analyzing the monitoring data of 72 anchor cables, the loss rate of anchor cables within 24 hours of tension locking, the loss

rate within 72 hours of tension locking, and the long-term loss rate of tension locking are shown in Tables 1–3.

Analyzing the monitoring data, the following can be obtained: the prestress loss within three days of tensioning accounts for about 75% of the long-term loss. The loss of the first and second rows is also different. The average loss rate of the second row is significantly lower than that of the first row.

3.2. Monitoring and Analysis of Anchor Cable Prestress Loss. Figure 5 shows the monitoring data from a first-row 750 kN anchor cable located at $K5+420$. The analysis of Figure 5 shows that the change in anchor cable prestress occurs in roughly three stages: (1) Day 0 (after locking) to Day 4, the rapid decline phase; (2) Day 5 to Day 14, the rise phase; and (3) after Day 14, a slightly fluctuating phase.

3.3. Initial Model Verification. Figure 5 shows the monitoring data from the first row of the 750 kN locked load cables in the K5 + 420 section, which was analyzed by linear regression. To this end, this study used $x = t$ and $y = -t/\ln(\omega(t))$ in the standard linear equation. Figure 6 shows a linear regression of the transformed data, and it was determined that $a = 4.283$ and $b = -0.891$ for these cables.

This process was repeated for the monitoring data from the first row of the 500 kN anchor cables at K5 + 365. Figure 7 shows the linear regression of the monitoring data for these cables, with $a = 8.534$ and $b = 4.399$.

However, with this model of prestress loss, several challenges remain. First, the prestress loss in the first three days was greater than in the remaining days; thus, accurate prediction of prestress loss over this period was difficult. Accordingly, this paper sought to ensure that the forecasted data for the first three days were accurate in subsequent iterations of the model. Second, on-site monitoring data may be missing due to a variety of reasons. Thus, this paper examined whether a small number of interval data points could be used to predict the entire prestress loss cycle.

3.4. Improved Model Analysis. The prestress loss rates of 52 prestressed anchor cables with a locked load of 750 kN and 20 prestressed anchor cables with a locked load of 500 kN over a 72 hour period to acquire additional data for model development were recorded. The average prestress loss for each locked load is shown in Table 4.

Table 4 shows that the average prestress loss of the anchor cable with a tensile load of 750 kN was 183.4 kN over the first three days. The average prestress loss of the anchor cable with a 500 kN tensile load was 68.8 kN over the first three days. From this information, a more ideal prediction model for the prestress loss over the first three days was identified such that

$$\left.\begin{aligned} F_{(3)} &= F_0 - \left(0.00036672F_0^2 - 22.88\right) \\ F_0 &\le 1500kN \end{aligned}\right\}, \tag{5}$$

where $F_{(3)}$ is the prestress value after three days and F_0 is the initial prestress. For cables where F_0 is greater than 1500 kN, further confirmation of the applicability of this model is required due to the large difference in load from the cables evaluated here.

Through the previously mentioned analysis, we determined the optimized prediction model to be

$$\left.\begin{aligned} F_3 &= F_0 - \left(0.00036672F_0^2 - 22.88\right) \longrightarrow t = 3 \\ F_{(t)} &= F_0\left[1 - \exp\left(-\frac{t}{at+b}\right)\right] \longrightarrow t \neq 3 \\ F_0 &\le 1500kN \end{aligned}\right\}. \tag{6}$$

Once the three unknown quantities of F_0, a, and b are identified, the anchor cable prestress loss over time can be determined. F_0 can be obtained after tensioning, and a and b were obtained from monitoring data. Reliable determination of these parameters is essential for the accuracy of this model.

Using the data in Figure 5 as an example, $t = \{1, 2, \ldots, 10\}$. Linear regression of this data was used to obtain $a = 3.442$ and $b = 2.707$. Using the first set of 750 kN anchor cables at K5 + 420 as an example and substituting $F_0 = 750$ kN, $a = 3.442$, $b = 2.707$ into equation (6), the prestress data were predicted according to the following equation:

$$F_{(t)} = 750\left[1 - \exp\left(-\frac{t}{3.442t + 2.707}\right)\right] \longrightarrow t \neq 3. \tag{7}$$

According to the data presented in Figure 8, the optimized model effectively predicts the long-term loss of anchor cable prestress. The actual monitoring data showed unstable fluctuations in the pretress values due to the influence of other factors, such as rainfall and construction.

3.5. Suitability Inspection and Model Validation

3.5.1. Inspection of Second-Row 750 kN Cables at K5 + 420. To test whether the model has universal applicability, the second row of the 750 kN cables at K5 + 420 was analyzed. According to the prediction model, $F_0 = 750$ kN and regression analysis of the data prior to $t = 10$ days revealed that $a = 2.2$ and $b = 4.828$. Substituting into equation (6), the prestress loss is predicted by equation (8) such that

$$F_{(t)} = 750\left[1 - \exp\left(-\frac{t}{2.2t + 4.828}\right)\right] \longrightarrow t \neq 3. \tag{8}$$

Figure 9 shows the comparison of the actual and predicted data for the second row 750 kN cables at K5 prediction model given by equation + 420.

Figure 9 shows that the prediction model is effective as it is in good agreement with the actual data. Through the analysis of multiple sets of anchor cables with a locked load of 750 kN, it was determined that the maximum difference between the predicted data and the measured data was less than 50 kN, and the error was between 0.04% and 8.9%.

Table 1: 24 h loss rate of anchor cable.

Anchor root number	Maximum loss rate (%)	Minimum loss rate (%)	Average loss rate (%)
72	15.93	2.94	9.56

Table 2: 72 h loss rate of anchor cable.

Anchor root number	Maximum loss rate (%)	Minimum loss rate (%)	Average loss rate (%)
72	32.78	6.09	21.46

Table 3: Long-term loss rate of anchor cable.

Anchor root number	Maximum loss rate (%)	Minimum loss rate (%)	Average loss rate (%)
72	46.41	10.31	28.30

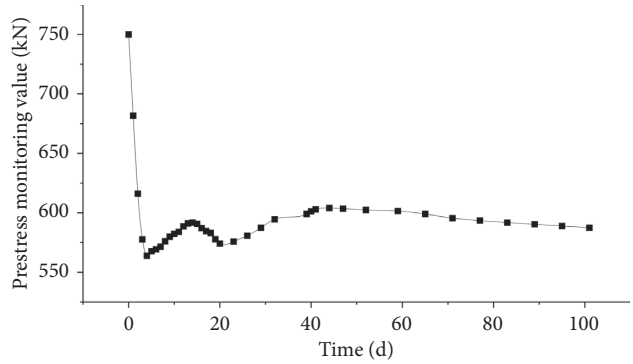

Figure 5: Prestress monitoring values for first-row 750 kN anchor cable located at K5 + 420.

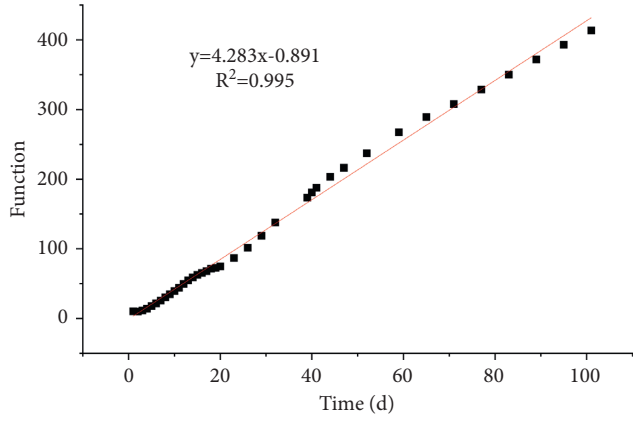

Figure 6: Linear regression of the prestress loss of the first row of 750 kN anchor cables at K5 + 420 over time.

3.5.2. Inspection of Second-Row 500 kN Cables at K5 + 365. For the second-row 500 kN cables located at K5 + 365, $F_0 = 500$ kN. Regression analysis of the monitoring data obtained prior to $t = 10$ days revealed that $a = 3.57$ and $b = 6.293$ for this cable. Substituting into equation (6), the predicted data was obtained (Figure 10) according to the following equation:

$$F_{(t)} = 500\left[1 - \exp\left(-\frac{t}{3.57t + 6.293}\right)\right] \longrightarrow t \neq 3. \quad (9)$$

By analyzing multiple datasets from anchor cables with a locked load of 500 kN, it was determined that the error of the model was between 0.04% and 8.9%. Therefore, compared with the preliminary model, the improved model overcomes the two major problems–namely, difficulty to predict prestress loss in the first three days and missing data, which can hinder prediction. The improved model, thus, provides more accurate and practical predictions for anchor cable prestress loss.

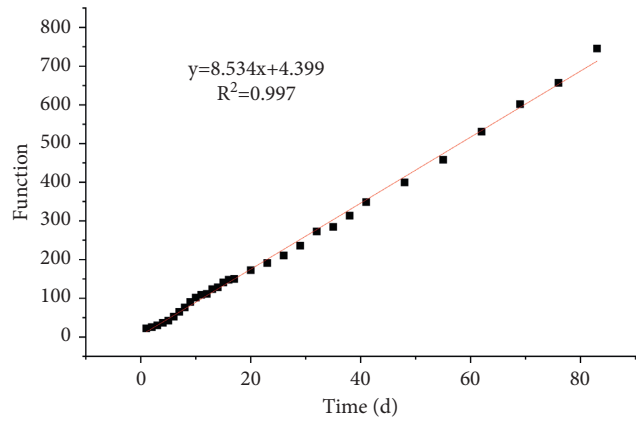

Figure 7: Linear regression of the prestress loss of the first row of 500 kN anchor cables at K5 + 365 over time.

Table 4: Average prestress loss of prestressed anchor cables over 72 h.

Locked load	750 kN (%)	500 kN (%)
Prestress loss within 72 h (% of locked load)	24.45	13.76

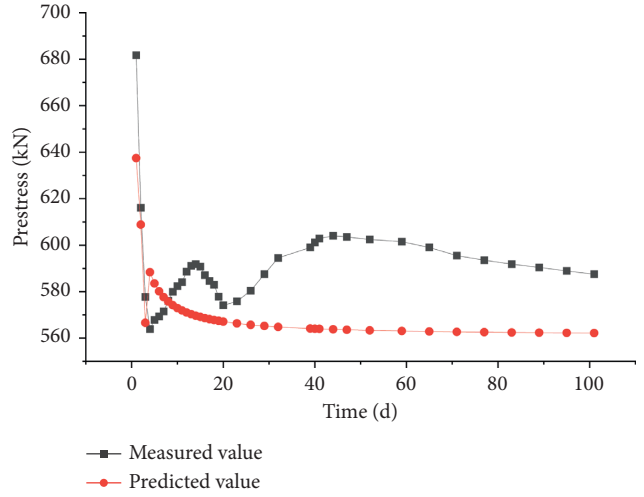

Figure 8: Comparison of measured data with improved model prediction data for the first row of 750 kN anchor cables at K5 + 420.

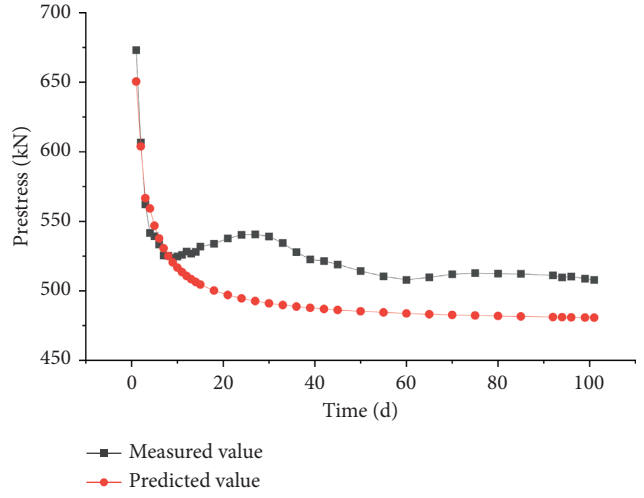

Figure 9: Comparison of measured and predicted data for the second row of 750 kN anchor cables at K5 + 420.

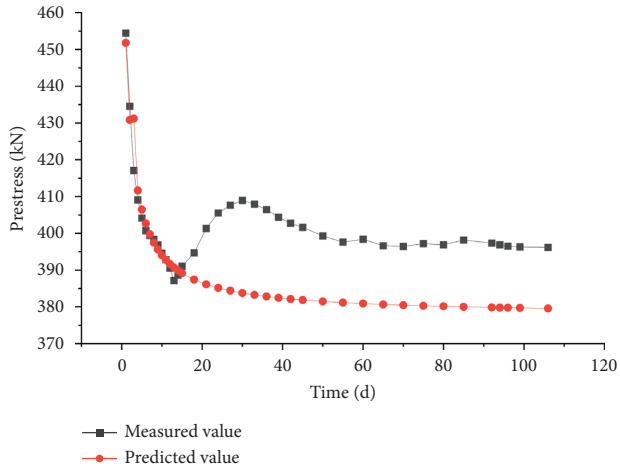

Figure 10: Comparison of measured and predicted data for the second row of 500 kN anchor cables at K5 + 365.

4. Discussion

The existing research on prestressed anchor cables has predominantly focused on the numerical analysis of the interaction mechanism of anchor cables and rock and soil masses and on the mechanical deformation of anchor cables. There are few studies on the dissipation of anchor cable prestress—an effect which has a significant impact on the quality, safety, and integrity of a construction or engineering project. The existing methods for determining the prestress loss of anchor cables are as follows. The first method is based on using existing monitoring data to summarize the prestress loss law and perform a qualitative analysis of loss characteristics. This method lacks generalizability and does not facilitate quantitative calculation. The second common method is based on laboratory tests, which are used to perform a full life cycle study of the prestressed anchor cables. However, this method is subjected to many ideal assumptions that are adopted to reduce the research area when implementing indoor models. The third method is a process analysis based on the numerical simulation method. This method requires a number of idealized assumptions, and the analysis of prestress loss over time has always been a major barrier to effective numerical simulation. In order to overcome the shortcomings of the previously mentioned methods, this paper used a regression analysis of on-site monitoring data and existing indoor research results to establish a mathematical model of anchor cable prestress loss over time based on comprehensive factors. This represents a significant improvement in modelling of anchor cable prestress loss compared with previous work. Furthermore, this study determined that the proposed model has broad applicability and the fundamental concept behind this model can be extended to other research methods. This statistics-based mathematical modelling and optimization approach overcomes many of the challenges associated with the accurate prediction of anchor cable prestress loss.

The main conclusions of the study are as follows. First, the loss of anchor cable prestress over time can be divided into three phases: the rapid decline phase after locking, the rise phase, and the stable phase. Second, the prestress loss of the anchor cable is related to rock mass creep, atmospheric precipitation, and construction methods, with rock mass creep being the most important factor. Based on these assumptions, the anchor cable prestress overtime can be expressed by a simple equation (equation (2)). Third, statistical data were used to improve the prestress loss model, to obtain the improved model (equation (6)), which effectively accounts for the accelerated prestress loss in the first three days. Furthermore, the improved model was obtained using a small amount of monitoring data, overcoming some of the challenges associated with lost or missing monitoring data. This model was used to accurately predict the characteristics of long-term prestress loss. The improved model had an error of 0.04% to8.9% between the predicted and measured values of anchor cable prestress. Thus, compared with the preliminary model, the improved model overcomes the two significant challenges of prestress loss being unpredictable in the first three days and being unable to predict prestress loss due to missing data.

5. Conclusions

In this study, a mathematical model for the prediction of anchor cable prestress loss was established based on monitoring data and regression analysis. This concept can also be extended to the analysis and modelling of other similar data. While this work has made a significant contribution to the quantitative modelling of prestress loss, a qualitative analysis of the interaction mechanism between the anchor cable and the rock and soil body remains to be explored. Finally, it is necessary to carefully consider the influence of rock mass creep, regional rainfall, and vibration on anchor cable prestress in order to create an effective prediction model of prestress loss.

Data Availability

The data used to support the findings of this study are available from the corresponding author upon request.

Conflicts of Interest

The authors declare that they have no conflicts of interest.

Acknowledgments

This work was supported by the National Natural Science Foundation of China (grant nos. 11872311 and 51708043), Natural Science Basic Research Plan in Shaanxi Province of China (grant no. 2019JQ-680), and Special Fund for Basic Scientific Research of Central Colleges (Natural Sciences) (grant no. 300102219209).

References

[1] N. Li, Y. Zhao, and Y. Han, "Mechanical model and numerical simulation test analysis of single anchor," *Journal of Xi'an University of Technology*, vol. 1, pp. 6–11, 1997.

[2] B. Brahim and G. Ballivy, "Five-year monitoring of load losses on prestressed cement-grouted road anchor," *Canada Geotechnique*, vol. 28, pp. 668–677, 1991.

[3] B. Brahim, C. Mohamed, and X. Haixue, "Long-term service behaviour of cement grouted anchors in the laboratory and field," in *Anchors Theory Practice*, Widmann, Ed., pp. 396–403, Balkema, Rotterdam, Netherlands, 1995.

[4] B. Xiao, "Preliminary analysis of prestress loss and anchoring effect of anchor cable of Three Gorges ship lock," *People's Changjiang River*, vol. 34, pp. 6-7, 2003.

[5] D. Li, P. Tang, and Y. Li, "Monitoring of prestressed rock anchor in phase I of three Gorges permanent ship lock," *Journal of Yangtze River Scientific Research Institute*, vol. 17, pp. 39–41, 2000.

[6] D. Ding and S. Bai, "Analysis of stress loss of rock mass reinforced by prestressed anchor cable," *Journal of Engineering Geology*, vol. 3, pp. 65–69, 1995.

[7] A. Chen, J. Gu, J. Shen, and Z. Ming, "Model test research on the law of tension tonnage of anchor cable in soft rock reinforcement with time," *Journal of Rock Mechanics and Engineering*, vol. 21, pp. 251–255, 2002.

[8] W. S. Zhu, B. Sui, X. J. Li, S. C. Li, and W. T. Wang, "A methodology for studying the high wall displacement of large scale underground cavern complexes and it's applications," *Tunnelling and Underground Space Technology*, vol. 23, no. 6, pp. 651–664, 2008.

[9] W. S. Zhu, X. J. Li, Q. B. Zhang et al., "A study on sidewall displacement prediction and stability evaluations for large underground power station caverns," *International Journal of Rock Mechanics and Mining Sciences*, vol. 47, no. 7, pp. 1055–1062, 2010.

[10] Y. Li, W. Zhu, J. Fu, Y. Guo, and Y. Qi, "A damage rheology model applied to analysis of splitting failure in underground caverns of Jinping I hydropower station," *International Journal of Rock Mechanics and Mining Sciences*, vol. 71, pp. 224–234, 2014.

[11] A. Wu, J. Wang, Z. Zhou et al., "Engineering rock mechanics practices in the underground powerhouse at Jinping I hydropower station," *Journal of Rock Mechanics and Geotechnical Engineering*, vol. 8, no. 5, pp. 640–650, 2016.

[12] K. Wang, H. Wu, and Y. Zhao, "Coupling between reduction of force in prestressed anchor cable and rock creep in deep-buried underground powerhouse," *Chinese Journal of Rock Mechanics and Engineering*, vol. 37, pp. 1481–1488, 2018.

[13] G. Chen, T. Chen, Y. Chen, R. Huang, and M. Liu, "A new method of predicting the prestress variations in anchored cables with excavation unloading destruction," *Engineering Geology*, vol. 241, pp. 109–120, 2018.

[14] Z. Tao and B. Pan, *Principles and Methods of Rock Mechanics*, China University of Geosciences Press, Wuhan, China, 1991.